

# Thermal Degradation Behavior of Poly(lactic acid) Stereocomplex

Yujiang Fan<sup>a,b</sup>, Haruo Nishida<sup>a\*</sup>, Yoshihito Shirai<sup>b</sup>, Yutaka Tokiwa<sup>c</sup>, and Takeshi Endo<sup>a,d</sup>

<sup>a</sup> Molecular Engineering Institute, Kinki University, 11-6 Kayanomori, Iizuka, Fukuoka 820-8555, Japan

<sup>b</sup> Graduate School of Life Science and Systems Engineering, Kyushu Institute of Technology, 1-1 Hibikino, Kitakyushu, Fukuoka 808-0196, Japan

<sup>c</sup> National Institute of Advanced Industrial Science and Technology (AIST), AIST Tsukuba Central 6, Tsukuba, Ibaraki 305-8566, Japan

<sup>d</sup> Faculty of Engineering, Yamagata University, 4-3-16 Jonan, Yonezawa, Yamagata 992-8510, Japan

\*Corresponding author: Haruo Nishida

Molecular Engineering Institute, Kinki University, Fukuoka 820-8555, Japan

Tel / Fax: +81-948-22-5706.

E-mail address: hnishida@mol-eng.fuk.kindai.ac.jp (H. Nishida)

## Abstract

Thermal degradation of poly(lactic acid) stereocomplex (scPLA) was investigated to clarify the pyrolysis mechanism. Three scPLA samples with different chain end structures were prepared, namely, as-polymerized scPLA-ap, precipitated-with-methanol scPLA-pr, and purified metal-free scPLA-H. From the analyses of thermal degradation kinetics and pyrolyzates of the scPLA samples, typical degradation mechanisms of these scPLAs were proposed as follows: The pyrolysis of scPLA-ap proceeds through main unzipping depolymerization caused by Sn-alkoxide chain ends with apparent  $E_a = 80\text{-}100 \text{ kJ mol}^{-1}$ , showing zero-order weight loss behavior. The pyrolysis of scPLA-pr also proceeds via a zero-order weight loss process consisting of main Sn-catalyzed selective lactide elimination with apparent  $E_a = 100\text{-}120 \text{ kJ mol}^{-1}$  caused by Sn-carboxylate chain ends. The pyrolyzates from scPLA-ap and scPLA-pr were predominantly L,L-/D,D-lactides. In the case of scPLA-H, random degradation is a main process, producing a large amount of *meso*-lactide and cyclic oligomers. These degradation mechanisms were nearly the same as those of the corresponding PLLAs, except that the scPLA-ap pyrolysis started at higher temperature due to the higher melting point of scPLA.

**Keywords:** poly lactide / poly (lactic acid) / stereocomplex / thermal degradation / thermal stability / pyrolysis / kinetics

## 1. Introduction

Poly(lactic acid) {poly(lactide), PLA} is one of the best-known bioabsorbable polymers and has received much interest for its medical and pharmaceutical applications [1-3]. It originates naturally from renewable resources, and has many good properties, such as biodegradability, mechanical strength, transparency, and compostability [4-6]. These properties have recently attracted both industry and academia, who believe that PLA and its related copolymers can substitute for commodity resins and take over many of their applications [7].

The optically pure poly(L-lactide) (PLLA) and poly(D-lactide) (PDLA), derived from L,L- and D,D-lactides, respectively, are crystal polymers having the same melting point at about 175°C [8]. Interestingly, in 1980s, it was found that an equivalent mixture of PLLA and PDLA formed a stereocomplex (scPLA), which had a higher melting point (245°C) than those of PLLA and PDLA alone [9,10]. Consequently, the stereocomplex has been extensively studied, especially regarding new synthetic approaches using a mixture of L,L-lactide and D,D-lactide in a simple and direct process [11-15]. Such studies, which progress the synthetic chemistry of scPLA, are expected to greatly extend its applications.

It is well known that PLA belongs to a group of polymers, which, because their repeated aliphatic ester structure is relatively easy to breakdown, are easy to hydrolyze and have poor thermal and photo-stability [16-18]. These characteristic properties of PLA are important in determining how molten scPLA should be processed without causing serious thermal decomposition.

Many studies on the thermal degradation and thermal stability of PLA have been reported. Factors, which influence the thermal behavior of PLA, include molecular weight and its distribution, residual and hydrolyzed monomers and oligomers, residual metal catalyst, and moisture, etc. McNeill and Leiper investigated the degradation of PLA under conditions of both controlled heating and isothermal heating [19,20]. They reported that the main products in the pyrolysis were cyclic oligomers, including lactides. They also determined the production of other lower boiling point products, such as carbon dioxide, acetaldehyde, ketene, and carbon monoxide. In their research, they employed a 1st-order reaction kinetic equation to calculate the apparent activation energy,  $E_a$ , as 119 kJ mol<sup>-1</sup>, in the temperature range of 240-270 °C. Kopinke and co-workers reported a multi step process for PLLA pyrolysis. They found that intra-molecular transesterification was a dominant degradation pathway, and that pyrolysis behavior was different between pure and Sn-containing PLLAs [21,22]. Cam et al. reported that some metal compounds, such as Sn, Zn, Al and Fe, had a great influence on the pyrolysis behavior of PLLA [23]. In 1999, Babanalbandi et al. [24] reported  $E_a$  values for PLLA pyrolysis using an isothermal method. They showed that the  $E_a$  value complexly changed as 103 ' 72 ' 97 kJ mol<sup>-1</sup> accompanied by a weight loss. Aoyagi et al. also reported a similar result of a complex change in  $E_a$  value (90 ' 80 ' 160 kJ mol<sup>-1</sup>) [25]. They reported that the pyrolysis of PLLA involved more than two mechanisms. Recently, we have presented one

solution for understanding the complex thermal degradation behavior of PLLA by analyzing the kinetics and mechanism of the thermal degradation of some PLLAs with a variety of end structures [26-29]. Consequently, we clarified that various degradation processes occurred each having individual kinetic parameters. The particular process and parameters depend on the PLLA's Sn content and end structure, as well as the temperature of pyrolysis. In explanation we proposed various types of degradation mechanisms dependant on the Sn content and end-structure, i.e., nucleophilic attack by alkoxide anion on carbonyl carbon, Sn-catalyzed selective lactide elimination, S<sub>N</sub>2 reaction on asymmetrical methyne carbon, and random degradation initiated by metal-free chain ends [27,29].

Despite there being so many reports on PLA pyrolysis, to date we are not aware of any report on the thermal degradation of scPLA having been published, although its melting properties have been intensively studied. The high melting point of scPLA has been the focus of many of its potential applications. The melt-processing of scPLA needs higher temperatures than that of PLLA, which means that it is important to determine the thermal degradation characteristic of scPLA in detail in order to control it. In this study, to clarify the thermal degradation behavior of scPLA, thermogravimetric analysis (TG/DTA) and pyrolysis-gas chromatography/mass spectrometry (Py-GC/MS) were applied to analyze pyrolyzates. Pyrolysis kinetics was also discussed based on the TG/DTA results, and a possible degradation mechanism was proposed.

## 2. Experimental part

### 2.1. Materials

Monomers, L,L- and D,D-lactides were obtained from Shimadzu Co. Ltd. and PURAC. These monomers were purified by recrystallization three times from dry toluene and then one time from dry ethyl acetate. After the purification, in each lactide, no other stereoisomer was detectable by gas chromatography (GC) measurement. The vacuum dried L,L- and D,D-lactides were stored in an N<sub>2</sub> atmosphere before use. A catalyst, tin 2-ethylhexanoate {Sn(Oct)<sub>2</sub>} was obtained from Wako Pure Chemical Industries, Ltd. and distilled under reduced pressure. Other chemicals and solvents were purchased from Wako Pure Chemical Industries, Ltd. and used as received.

### 2.2. Polymerization of L,L- and D,D-lactides

Both PLLA and PDLA were synthesized by ring-opening polymerization of L,L- and D,D-lactides catalyzed by Sn(Oct)<sub>2</sub> in bulk, respectively. Purified L,L- or D,D-lactide 1.0 g (6.94 mmol) was added into a reaction tube in a glove box under N<sub>2</sub> atmosphere. A solution of 0.2M Sn(Oct)<sub>2</sub>/toluene 17.3 μL (3.47 μmol) was added by using a micro syringe. The reaction tube was connected to a vacuum line and the toluene was evaporated for 48 h at ambient temperature *in vacuo*.

After the tube was flame sealed, it was immersed into an oil bath and heated according to a multi-temperature process (150 °C/0.5 h + 130 °C/5 h + 110 °C/13 h + 90 °C/12 h). After the polymerization, white solid as-polymerized PLA (PLLA-ap or PDLA-ap) was obtained. According to <sup>1</sup>H-NMR analysis, both the polymerization of L,L- and D,D-lactides proceeded with ~100 % conversion.

A part of the as-polymerized PLA was dissolved in chloroform and precipitated with 10-fold of methanol to prepare a precipitated PLA (PLLA-pr or PDLA-pr) in about 95 % yield. Further, a part of the precipitated PLA was dissolved in chloroform, then residual Sn compounds in the PLA were extracted with 1M HCl aqueous solution three times, after which the chloroform solution was washed with distilled water until the aqueous phase became totally neutral. Finally, the polymer was precipitated with methanol to prepare the purified PLA (PLLA-H or PDLA-H) in about an 80 % yield.

### 2.3. Preparation of PLLA/PDLA stereocomplex (scPLA) film

For preparing scPLA film samples, equal amounts of PLLA and PDLA were dissolved in chloroform (0.05 g each in 5 mL CHCl<sub>3</sub>) and then cast on a glass Petri dish surface. After evaporation of the solvent, formed film was washed by methanol and then vacuum dried to obtain an scPLA film sample (scPLA-ap, scPLA-pr, or scPLA-H).

### 2.4. Dynamic pyrolysis

Thermogravimetric analysis (TG/DTA) of scPLA film samples was conducted on a Seiko Instruments Inc. EXSTAR 6200 TG system in aluminum pans under a constant nitrogen flow (100 mL min<sup>-1</sup>) using about 5 mg of scPLA film sample. For each sample, prescribed heating rates,  $\phi$ , of 1, 3, 5, 7, and 9 K min<sup>-1</sup> were applied from room temperature to 400°C. The pyrolysis data were collected at regular intervals (about 20 times K<sup>-1</sup>) by an EXSTAR 6000 data platform, and recorded into an analytical computer system.

### 2.5. Isothermal pyrolysis of scPLA in glass tube oven

About 50 mg of scPLA-ap sample was put into a Shibata GTO-350D glass tube oven. After air was substituted by nitrogen in the chamber of the oven, the oven was heated rapidly to 250°C and then kept at this temperature for 2h. The distilled components were collected and analyzed by gas chromatography (GC).

### 2.6. Measurements

<sup>1</sup>H-NMR spectra were recorded on a Varian INOVA400 NMR spectrometer operating at 400 MHz for a proton investigation in chloroform-*d* solution with tetramethylsilane as the internal

standard.

The gas chromatography (GC) measurements were recorded on a Shimadzu GC-9A gas chromatograph with a Varian cyclodextrine-2-236M-19 capillary column (0.25 mm × 50 m) using helium as a carrier gas. The column and injector were set isothermally at 150 and 220 °C, respectively. The sample (3 mg) was dissolved in acetone (1 mL) and a 1 µL aliquot of the solution was injected. The peaks for *meso*-, L,L-, and D,D-lactides were identified by comparison with pure substance peaks.

Differential scanning calorimetry (DSC) measurements were carried out under a nitrogen flow of 20 mL min<sup>-1</sup> using a SEIKO Instruments Inc. EXSTAR6000-DSC6200 calibrated with indium. The film samples (2-3 mg) were encapsulated in aluminum pans and heated from 30 to 250 °C at a heating rate of 10 °C min<sup>-1</sup>. The first, second, and third scans were recorded in all cases. The melting temperature ( $T_m$ ) was taken at the peak point.

Gel permeation chromatography (GPC) was measured on a TOSOH HLC-8220 GPC system at 40°C using TOSOH TSKgel Super HM-H column and chloroform eluent (0.6 mL min<sup>-1</sup>). Low polydispersity polystyrene standards with  $M_n$  from  $5.0 \times 10^2$  to  $1.11 \times 10^6$  were used for calibration. The PLLA or PDLA sample (12 mg) was dissolved in chloroform (2 mL) before filtering the solution through a 0.5 µm membrane filter.

The Sn content in scPLA samples was measured with a Shimadzu ICPS-8000 interactively coupled plasma spectrometer (ICP). The sample was degraded by a 25 % ammonia solution, diluted with 1M-HCl, and then measured.

Pyrolysis-gas chromatograph/mass spectra (Py-GC/MS) were recorded on a Frontier Lab double-shot pyrolyzer PY-2020D with a Frontier Lab SS-1010E selective sampler connected to a Shimadzu GCMS-QP5050 chromatograph/mass spectrometer. High purity helium was used as carrier gas at 50 mL min<sup>-1</sup>. The volatile products were analyzed with an Ultra Alloy<sup>+</sup>-5 capillary column (30 m × 0.25 mm i.d.; film thickness, 0.25 µm). The film sample was put in the pyrolyzer and heated from 60 °C to a prescribed temperature at a heating rate of 10 °C min<sup>-1</sup>. The volatile pyrolysis products were introduced into the GC through the selective sampler. The temperature of the column oven was first set at 40°C. After the pyrolysis process had finished, the column was heated according to the following program: 40 °C for 1 min; 40-120 °C at 5 °C min<sup>-1</sup>; 120-320 °C at 20 °C min<sup>-1</sup>; 320 °C for 13 min. Mass spectrum measurements were recorded 2 times s<sup>-1</sup> during this period.

## Results and discussion

### 3.1. Preparation of PLA stereocomplex

Original PLLA and PDLA were synthesized through the ring-opening polymerization of L,L- and D,D-lactides, respectively, using tin 2-ethylhexanoate {Sn(Oct)<sub>2</sub>} as a catalyst in bulk. In this

equilibrium polymerization system [30], a solid phase polymerization was employed for a long time (13 h/110 °C + 12 h/90 °C) to minimize the presence of residual lactide in the product [31]. From <sup>1</sup>H-NMR and GPC analyses of as-polymerized PLAs (PLLA-ap and PDLA-ap), no residual lactide was detected in each PLA. According to Kowalski et al. [32], it is assumed that Sn atoms in the as-polymerized PLAs bond through alkoxide groups to polymer chain ends to form “PLA-O-Sn”. The as-polymerized PLAs were dissolved in chloroform and precipitated with excess methanol to prepare precipitated PLAs (PLLA-pr and PDLA-pr). During the precipitation process, the end structure “PLA-O-Sn” will change into “PLA-OH” by a reaction with excess methanol [33]. According to the previous reports [23,34,35], Sn atoms in PLA are not removable from the polymer matrix even through a repeated precipitation process. It is considered that after the precipitation process Sn atoms in the precipitated PLAs must be bonded to polymer chain ends in the form of a salt, “HO-PLA-COO<sup>-</sup> Sn<sup>2+</sup>X<sup>+</sup>”. Further, to prepare the metal free polymer “HO-PLA-COOH”, the precipitated PLAs were treated by a liquid-liquid extraction method with 1M HCl [22,23,26], resulting in the formation of purified PLAs (PLLA-H and PDLA-H).

Characteristics of the three sets of PLAs are listed in Table 1. All PLAs had nearly the same molecular weight of  $M_n$  118,000-128,000 and  $M_w$  207,000-220,000. From DSC analysis, observed high  $T_m$  values (178-179 °C) of PLLA-H and PDLA-H indicate the sufficient optical purity of the PLAs.

**Table 1.** PLA and scPLA samples

Sample description	PLAs			scPLAs			
	$T_m$ (°C)	$M_n$	$M_w$	$T_m$ (°C)	$\Delta H$ (J/g)	Sn content (ppm)	
As-polymerized	PDLA-ap	124,000	212,000	scPLA-ap	236.6	58.2	286
	PLLA-ap	118,000	209,000				
Precipitated with methanol	PDLA-pr	124,000	210,000	scPLA-pr	237.2	64.7	266
	PLLA-pr	120,000	211,000				
Purified with 1M HCl aq.	PDLA-H	179.5	220,000	scPLA-H	236.9	56.9	< 10
	PLLA-H	178.7	207,000				

To prepare the stereo complex samples, each set of PLAs with equal amounts of corresponding PLLA and PDLA was dissolved in chloroform and then cast on the glass surface. Evaporation of the solvent gave transparent scPLA film samples (Table 1). Tin contents of scPLAs were measured with ICP, and found to be scPLA-ap, 286 ppm; scPLA-pr, 266 ppm; and scPLA-H, <10 ppm. This last value indicates that the amount of Sn in scPLA-H was below the lower limit of detection under the experimental conditions. As is well known, scPLAs have different thermal properties from the original PLAs as shown in Table 1. Representative DSC spectra of scPLA-H film are illustrated in Figure 1. As-cast scPLA film showed a higher  $T_m$  value, at about 240 °C in first scan, than those of PLLA-H and PDLA-H. After the melting, the sample was quenched at -74 °C by

dry ice/methanol, and then given a second scan. A DSC spectrum of the second scan showed a clear  $T_g$  transition point at 56 °C, a crystallization peak at 120~140°C, followed by two melting peaks at around 175°C and 230°C. A third scan was carried out after the second scanned sample had been left standing to cool, which showed similar  $T_m$  peaks to the second scan, but no crystallization peak was detected. According to the previous reports [9,11], the as-cast scPLA films must be mainly composed of typical stereocomplex crystal having  $T_m$  at about 240°C. On the other hand, the crystallized scPLAs in molten state had two kinds of crystal regions, i.e., homochiral crystals and stereocomplex crystal regions. In this paper, the as-cast scPLA films were used for the following studies.

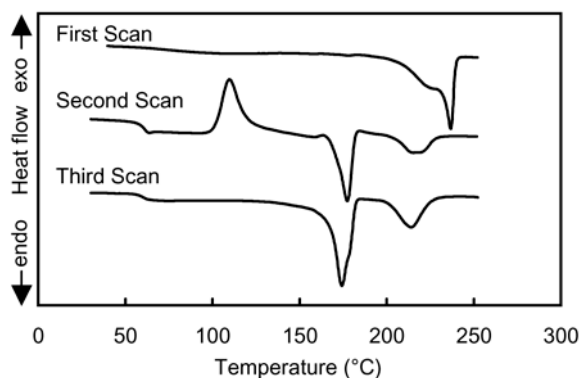


**Figure 1.** DSC curves of scPLA-H at a heating rate of 10 K min<sup>-1</sup> under N<sub>2</sub> flow of 20 ml min<sup>-1</sup>. First scan: as-casting film; second scan: quenched sample after first scan; third scan: normally cooled sample after second scan.

The three as-cast scPLA films had nearly equal  $T_m$  and  $H$  values, but different Sn content values (Table 1). According to the previous report on the effect of residual Sn atoms in PLLA pyrolysis [28], the Sn content values of scPLA-ap (286 ppm) and scPLA-pr (266 ppm) samples are regarded as having nearly equal values. Thus, differences in the thermal degradation behavior among the three scPLA samples must reflect the differences in the polymer chain end structures, “scPLA-O-Sn”, “HO-scPLA-COO<sup>-</sup> Sn<sup>2+</sup>X<sup>+</sup>”, and “HO-scPLA-COOH”, without any need to consider the influences of molecular weight and crystal structure.

### 3.2. Thermogravimetric analysis (TG) of scPLAs

Thermogravimetric analysis (TG) is an effective approach for evaluating the thermal properties of polymer materials. To analyze the thermal degradation behavior of scPLA samples, a dynamic thermal degradation procedure was conducted with TG/DTA in nitrogen flow. Typical weight loss profiles of scPLA samples at  $\phi = 5$  K min<sup>-1</sup> are shown in Figure 2, compared to the profiles of corresponding PLLA and PDLA samples.

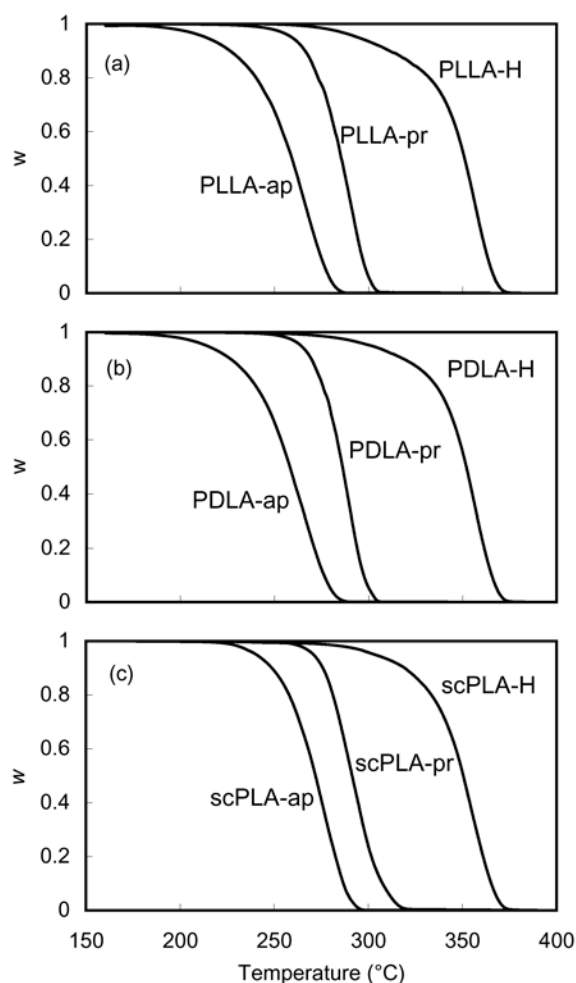


**Figure 2.** Thermogravimetric curves of (a) a set of PLLAs, (b) PDLAs, and (c) scPLAs at a heating rate of  $5 \text{ K min}^{-1}$  under  $\text{N}_2$  flow of  $100 \text{ ml min}^{-1}$ .

Results in Figure 2(a) were nearly the same as previously reported TG profiles of a set of PLLA samples ( $M_n$  217,000-266,000;  $M_w$  429,000-451,000; Sn content, 1,006 (ap), 689 (pr), 23 ppm (H)) [29]. These indicate that the thermal degradation behavior of PLLA samples can be readily reproduced. The TG profiles of a set of PDLA samples (Figure 2(b)), which were first shown in this study, completely agreed with the profiles of corresponding PLLA samples. This means that both homopolymers degrade in the same manner under the same conditions without being influenced by optical isomerism.

In the cases of scPLA samples, each sample showed an individual TG curve in a different temperature range (Figure 2(c)). The weight loss of scPLA-ap started at around  $220 \text{ }^\circ\text{C}$  and finished at around  $290 \text{ }^\circ\text{C}$ . The weight loss of scPLA-pr started at a higher temperature of around  $260 \text{ }^\circ\text{C}$  and rapidly proceeded to completion at around  $320 \text{ }^\circ\text{C}$ . In the case of scPLA-H, the degradation occurred in the highest temperature range, starting at around  $260 \text{ }^\circ\text{C}$  and finishing at around  $380 \text{ }^\circ\text{C}$ . The

differences in thermal degradation behavior among these scPLA samples are obvious, i.e., scPLA-ap and scPLA-pr degraded in a narrow temperature range of about 60-70 °C, whereas the pyrolysis of scPLA-H continued to degrade through a wide temperature range of 120 °C. The individual TG profile of each scPLA sample must be ascribed to a characteristic degradation mechanism occurring in a particular temperature range, rather than a simple downward shift of the degradation temperature range with the Sn content, since both scPLA-ap and scPLA-pr have almost the same Sn content. Thus, these characteristic degradation behaviors should be due to the different chain end structures, which must initiate different degradation reactions.

Comparing the TG profiles of scPLAs with those of PLLAs and PDLAs showed the profiles of scPLA-pr and scPLA-H to be nearly same as those of corresponding PLLA and PDLA samples. In contrast, the profile of scPLA-ap showed a shift to a temperature range higher than those of PLLA-ap and PDLA-ap, especially for temperature ranges where the starting temperature was higher than 40°C. The major reason for this difference is the higher melting point of scPLA compared to those of PLLA and PDLA. In Figure 3, DTA profiles of scPLA-ap and PLLA-ap are illustrated along with the TG profiles. The  $T_m$  peaks of scPLA-ap and PLLA-ap were observed at around 240 °C and 180 °C, respectively, which corresponded to the starting points of the weight loss in TG profiles. Thus, these results mean that the thermal degradation of scPLA starts at a temperature above its  $T_m$ , even in the presence of Sn compound as a degradation catalyst. Obviously, the thermal degradation of PLAs was affected by the  $T_m$  of the crystal, because of the restricted mobility of molecular chains in the crystals.

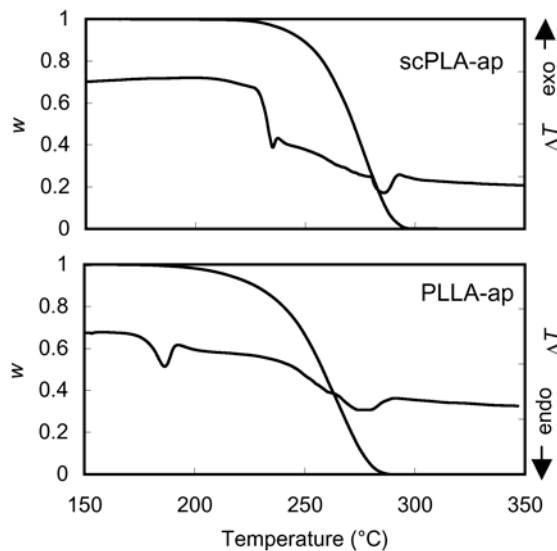


**Figure 3.** TG/DTA curves of scPLA-ap and PLLA-ap pyrolysis at a heating rate of 5 K min<sup>-1</sup> under N<sub>2</sub> flow of 100 ml min<sup>-1</sup>.

### 3.3. Activation energy of scPLA pyrolysis

The apparent activation energy,  $E_a$ , of the thermal degradation of scPLAs was estimated from the weight loss data according to a previously published method [36-39]. The TG measurement was carried out at various heating rates  $\phi$  of 1~9 K min<sup>-1</sup>, and then the  $E_a$  values were calculated with plural methods [36,37,40]. Figure 4 shows the  $E_a$  values at different fractional weights,  $w$ , during the pyrolysis of scPLA-ap, scPLA-pr, and scPLA-H. Each sample exhibits a characteristic  $E_a$  curve. The  $E_a$  value of scPLA-ap decreased gradually from 100 to 80 kJ mol<sup>-1</sup> with  $w$ . This change in  $E_a$  value closely followed the  $E_a$  curve of PLLA-ap pyrolysis obtained in our previous study [29]. Wachsen et al. also reported a similar  $E_a$  value of 92 kJ mol<sup>-1</sup> for the pyrolysis of as-polymerized PLLA catalyzed by Sn(Oct)<sub>2</sub>, though they calculated the  $E_a$  value from the change in molecular weight, regarding it as a random decomposition reaction [41]. In the case of scPLA-pr, which had a similar Sn content with that of scPLA-ap, the  $E_a$  value decreased from 120 to 100 kJ mol<sup>-1</sup>, keeping about 20 kJ mol<sup>-1</sup> higher than that of scPLA-ap. This result is comparable with  $E_a$  H 120 kJ mol<sup>-1</sup> of PLLA-pr samples containing 169-607 ppm of Sn atom in the previous report [28]. Obviously, the gap in  $E_a$  value between scPLA-ap and scPLA-pr pyrolysis is significant, and corresponds to the gap in the degradation temperature range. This must reflect any differences that exist in the pyrolysis mechanism of each sample. The  $E_a$  value of scPLA-H, which started at about 125 kJ mol<sup>-1</sup> and rose up to 180 kJ mol<sup>-1</sup> as the degradation progressed, agrees with the previously reported values for purified PLLA-H [26,28]. These results indicate that the scPLA degrade through a similar reaction route to those of the corresponding PLLA.

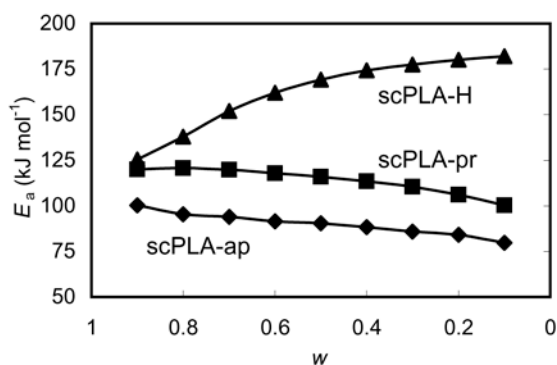


**Figure 4.** Apparent activation energy,  $E_a$ , values of scPLA-ap, scPLA-pr, and scPLA-H pyrolysis.

### 3.4. Kinetics of scPLA pyrolysis

The thermal degradation kinetics of scPLA samples was studied by several analytical approaches [38,42,43]. Integration analysis plots of TG data of scPLA-ap (5 K min<sup>-1</sup>) and model reactions are shown in Figure 5, in which activation energy value  $E_a = 90$  kJ mol<sup>-1</sup> and

pre-exponential value  $A = 1.0 \times 10^6 \text{ s}^{-1}$  were employed. In this Figure,  $\theta = (E_a/\phi R)p(y)$  is defined as the reduced time [38], where  $R$  is the molar gas constant and function  $p(y)$  is tabulated by Doyle [40]. After a slow weight loss process in the initial period, the experimental data plot showed an almost linear relationship between  $w$  and  $A_j$  in parallel to a simulation plot of a zero-order reaction. In a later period, the experimental data plot curved slightly to the retarding side. As shown in Figure 4, the  $E_a$  value gradually changed with  $w$ . It is assumed that plural reactions were occurring during the pyrolysis of scPLA-ap, in which each reaction changed its contribution to the weight loss process with temperature. Thus, considering the Wachsen's speculation [18], a minor random degradation process may occur at the same time as the unzipping depolymerization, contributing to the resulting zero-order weight loss behavior. In the final stage of the pyrolysis, the experimental data plot gradually deviated from the simulation plot of the zero-order reaction, suggesting a gradual shift to a 1<sup>st</sup>-order or random degradation mechanism.

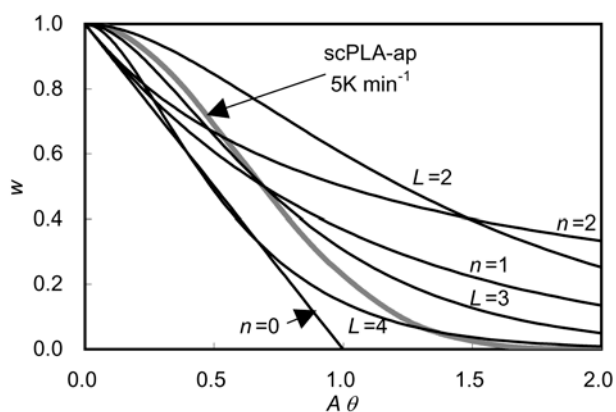


**Figure 5.** Plots of experimental  $(AE_a/\phi R)p(y)$  ( $=A\theta$ ) vs.  $w$  of scPLA-ap pyrolysis at a heating rate of  $5 \text{ K min}^{-1}$ , and of model reactions ( $E_a = 90 \text{ kJ mol}^{-1}$  and  $A = 1.0 \times 10^6 \text{ s}^{-1}$ ). Model reactions: zero- ( $n = 0$ ), 1st- ( $n = 1$ ), and 2nd-order ( $n = 2$ ), and random degradations ( $L = 2-4$ ).

In Figure 6, the experimental data of scPLA-pr pyrolysis ( $5 \text{ K min}^{-1}$ ) was plotted by the integral analysis method along with the simulation plots of model reactions with  $E_a = 115 \text{ kJ mol}^{-1}$  and  $A = 1.4 \times 10^8 \text{ s}^{-1}$ . Similar to the scPLA-ap pyrolysis, after a slow weight loss process in the initial period the experimental data plot showed a linear relationship between  $w$  and  $A_j$  in parallel to the simulation plot of a zero-order reaction. Thus, the main degradation of scPLA-pr was also a zero-order weight loss process. The initial slow weight loss process may have been caused in part by a lower mobility of long chain ends remaining in the initial period. Nearly the same result was found in the pyrolysis of PLLA-pr in our previous study [29]. Though the main degradation process of both scPLA-ap and scPLA-pr was evaluated as being the same zero-order weight loss process, each elementary reaction will be different because of the significant gaps in the kinetic parameters and

degradation temperature ranges.

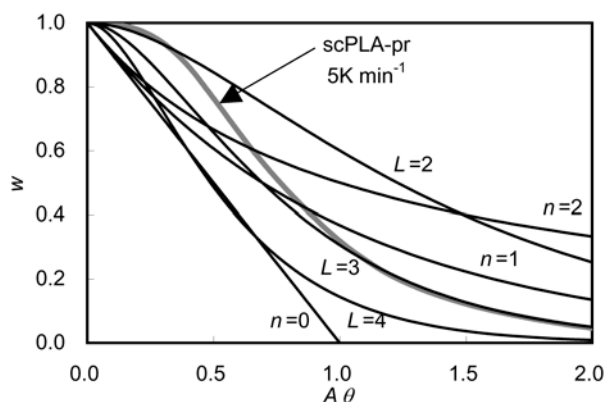


**Figure 6.** Plots of experimental  $(AE_a/\phi R)p(y)$  ( $=A\theta$ ) vs.  $w$  of scPLA-pr at a heating rate of 5 K min<sup>-1</sup>, together with model reactions ( $E_a = 115$  kJ mol<sup>-1</sup> and  $A = 1.4 \times 10^8$  s<sup>-1</sup>). Model reactions: zero- ( $n = 0$ ), 1st- ( $n = 1$ ), and 2nd-order ( $n = 2$ ), and random degradations ( $L = 2-4$ ).

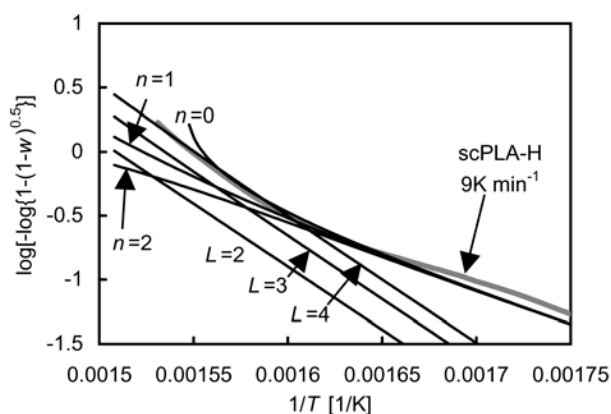


**Figure 7.** Plots of  $\log[-\log\{1-(1-w)^{1/2}\}]$  vs.  $1/T$  for thermogravimetric data of scPLA-H at a heating rate of 9 K min<sup>-1</sup>, together with model reactions ( $E_a = 178$  kJ mol<sup>-1</sup> and  $A = 2.0 \times 10^{12}$  s<sup>-1</sup>). Model reactions: zero- ( $n = 0$ ), 1st- ( $n = 1$ ), and 2nd-order ( $n = 2$ ), and random degradations ( $L = 2-4$ ).

The pyrolysis of scPLA-H was analyzed using the improved random degradation analysis method [43], which traced precisely the degradation routes of purified PLLA pyrolysis [26]. In Figure 7, the plots of  $\log[-\log\{1-(1-w)^{0.5}\}]$  vs.  $1/T$  for experimental data of scPLA-H (9 K min<sup>-1</sup>) and model reactions with kinetic parameters  $E_a = 178$  kJ mol<sup>-1</sup> and  $A = 2.0 \times 10^{12}$  s<sup>-1</sup> are illustrated. In this Figure, the data measured at  $\phi = 9$  K min<sup>-1</sup> were used to inspect the degradation path at the main stage of  $w < 0.5$ . This range is large enough to minimize the influence of minor reactions evident at a lower temperature range. The experimental data plot of scPLA-H closely followed the  $n$ th-order

reaction plots in the initial stages, and then shifted onto a random degradation simulation plot with  $L = 4-5$  in the later stages, where  $L$  means the least number of repeating units of oligomer not volatilized [38]. It was exactly the same with the degradation behavior of metal free PLLA-H as previously reported [26,28].

Therefore, the thermal degradation of each scPLA sample proceeded through characteristic plural reactions having peculiar kinetic parameters. Compared with the corresponding PLLA samples previously reported [29], almost the same thermal degradation behaviors and similar kinetic parameters were derived, except that the pyrolysis of scPLA-ap started at a temperature about 40 °C higher than that of PLLA-ap pyrolysis.

### 3.5. Pyrolyzates from scPLAs

It is well known that the 6-membered cyclic dimers, including *meso*-lactide, L,L-lactide and D,D-lactide, are the main ingredients in pyrolyzate of PLA [22,44,45]. Here, the pyrolyzates from the scPLA samples were analyzed to confirm the effects of the end-structures of scPLAs. Figure 8 shows Py-GC/MS chromatograms of pyrolyzates from scPLA-ap, scPLA-pr, and scPLA-H in a temperature range of 60-400 °C at a heating rate of 10 °C min<sup>-1</sup>. All samples showed a main peak at 13.4-13.7 min in retention time. This peak has been confirmed to be L,L-/D,D-lactides by comparing it with those of the standard substances [26,28]. Evolution of *meso*-lactide was clearly determined by a peak at 12.2 min in the chromatograms of scPLA-pr and scPLA-H, but this peak was only slightly visible in the chromatogram of scPLA-ap. Though the pyrolysis of PLLA-pr hardly formed any *meso*-lactide in our previous study [29], a small amount of *meso*-lactide (9.14 %) was formed in the pyrolysis of scPLA-pr. This difference between scPLA-pr and PLLA-pr could be attributable to the presence of PDLA component in scPLA-pr. The chromatogram of PLLA-H showed the formation of a large amount of *meso*-lactide (19.99 %) and other cyclic oligomers (32.01 %). A series of peaks periodically appearing in groups at 23-33 min represent the production of the cyclic oligomers from trimer to octamer, each of which consisted of a group of diastereoisomers [22,26,28,44].

Composition of L,L- and D,D-lactides in the pyrolyzates from scPLA was determined through the GC analysis with a capillary column, cyclodextrin-<sup>2</sup>-236M-19, to split diastereoisomers of the pyrolyzates. In Figure 9, a GC chromatogram of the pyrolyzates on the isothermal degradation of scPLA-ap at 250 °C for 2 h in a glass tube oven showed the formation of a nearly equal amount of L,L- (48.94 %) and D,D-lactides (48.71 %) at 12.4 and 13.1 min, respectively, and a small amount of *meso*-lactide (2.35 %). Thus, this means that the main peak at 13.4-13.7 min in Py-GC/MS chromatograms (Figure 8) is composed of an equal amount of L,L- and D,D-lactides.

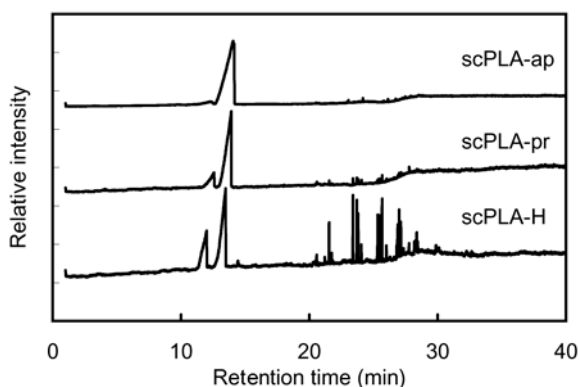


**Figure 8.** Py-GC/MS (TIC) chromatograms of scPLA-ap, scPLA-pr, and scPLA-H pyrolyzates in a heating process of 60-400°C at a constant heating rate of 10 K min<sup>-1</sup> under He flow of 50 ml min<sup>-1</sup>.

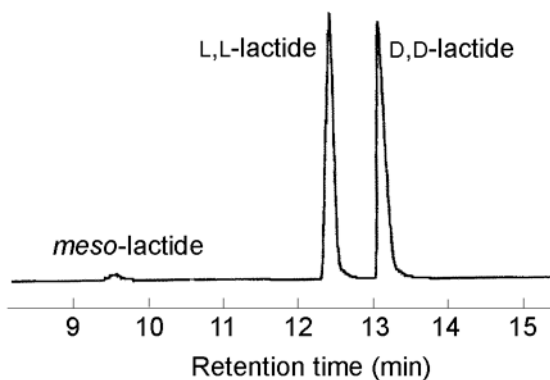


**Figure 9.** GC chromatogram for volatile pyrolyzates of scPLA-ap at 250 °C for 2 h in a glass tube oven.

To determine changes in the pyrolyzate composition, the pyrolyzates that had evolved in different temperature ranges from scPLAs were collected and analyzed with Py-GC/MS. Results of the composition analysis are illustrated in Figure 10, in which the content of each component was calculated from the corresponding peak intensity in the Py-GC/MS chromatogram. The pyrolyzates from scPLA-ap were, other than a small amount of *meso*-lactide (<5 %), almost all L,L-/D,D-lactides over the whole degradation range. The *meso*-lactide formation, after its appearance at 250 °C, gradually increased with temperature. On the other hand, the pyrolyzates from scPLA-pr were composed of the dominant L,L-/D,D-lactides and a greater amount of *meso*-lactide at temperatures higher than 280 °C. Interestingly, at lower temperatures than 270 °C, no *meso*-lactide formation was detected. The result that showed *meso*-lactide formation occurring at lower temperatures in scPLA-ap pyrolysis compared to scPLA-pr pyrolysis is similar to the result found in PLLA-ap and PLLA-pr pyrolysis [29]. It is considered that the *meso*-lactide formation is related to irregular

reactions occurring in later stages of the pyrolysis, and that such reactions should occur at higher temperatures in the case of scPLA-pr pyrolysis than scPLA-ap pyrolysis. The large amount of *meso*-lactide formation, compared to that formed in the PLLA pyrolysis, must be caused by some inter-molecular reactions between PLLA and PDLA chains in the later stage.

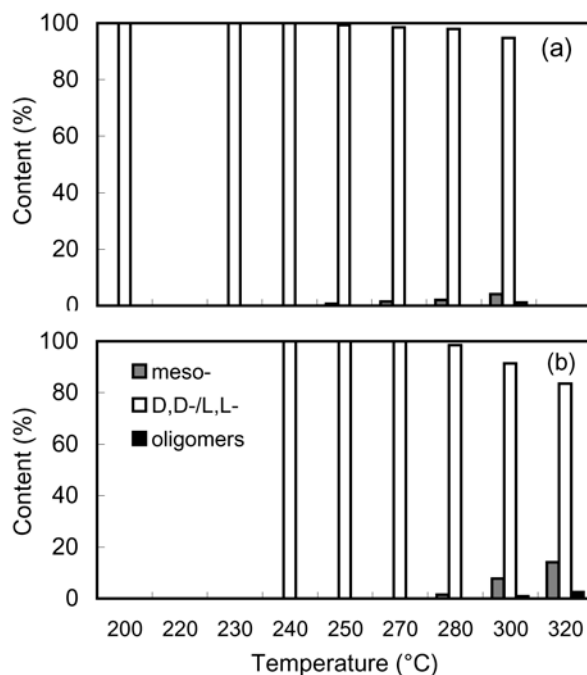
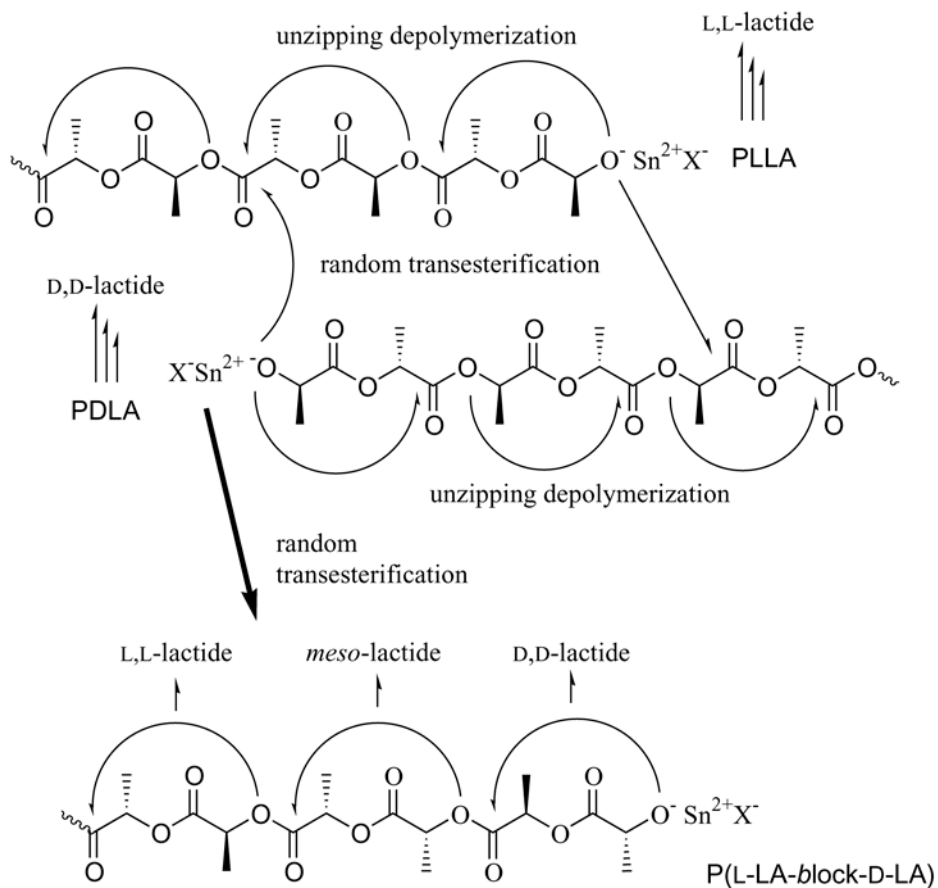


**Figure 10.** Content ratio of volatile products from scPLA-ap and scPLA-pr pyrolysis in different temperature ranges.

### 3.6. Mechanism of scPLA pyrolysis

The Sn-catalyzed polymerization of L,L- or D,D-lactide is a typical equilibrium polymerization [30,46]. It is considered that the thermal degradation of scPLA-ap proceeds in a similar way to the depolymerization mechanism in the equilibrium polymerization of L,L-/D,D-lactides (Scheme 1) [33]. Namely, the active end structure of scPLA-ap will be Sn-alkoxide with the alkoxide anion attacking a carbonyl carbon in a penultimate lactate unit, resulting in the formation of lactide [32,47]. This nucleophilic attack must occur repeatedly as an unzipping depolymerization to form the 6-membered cyclic dimer L,L- or D,D-lactide, so preventing the formation of *meso*-lactide. However, at a lower level other inter-molecular reactions such as bimolecular transesterification must occur to form some hetero-sequence units such as L-lactate-D-lactate in newly combined PLLA-PDLA chains, leading to the formation of a small amount of *meso*-lactide. Kowalski et al. estimated that the ratio of the rate constant for the polymerization,  $k_p$ , and bimolecular transesterification,  $k_{tr2}$ , on solution polymerization of L,L-lactide was 200 at 80 °C [33]. This bimolecular transesterification reaction

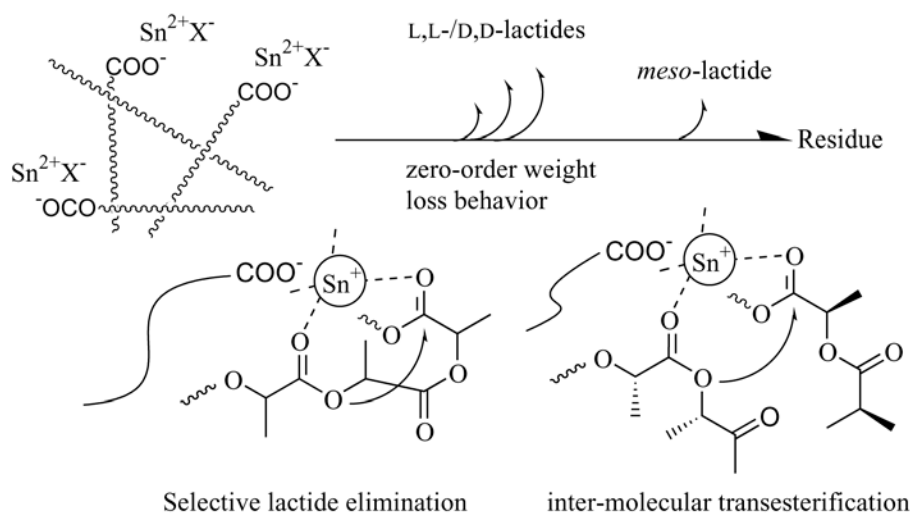
should occur more often at the later stage of pyrolysis, when a greater number of residual chains are concentrated around a chain end. This will be one reason for the increase in *meso*-lactide content at the later stage. Moreover, the observed zero-order weight loss behavior will be the result of a combination of the main unzipping depolymerization and the minor bimolecular transesterification reaction (Scheme 1).



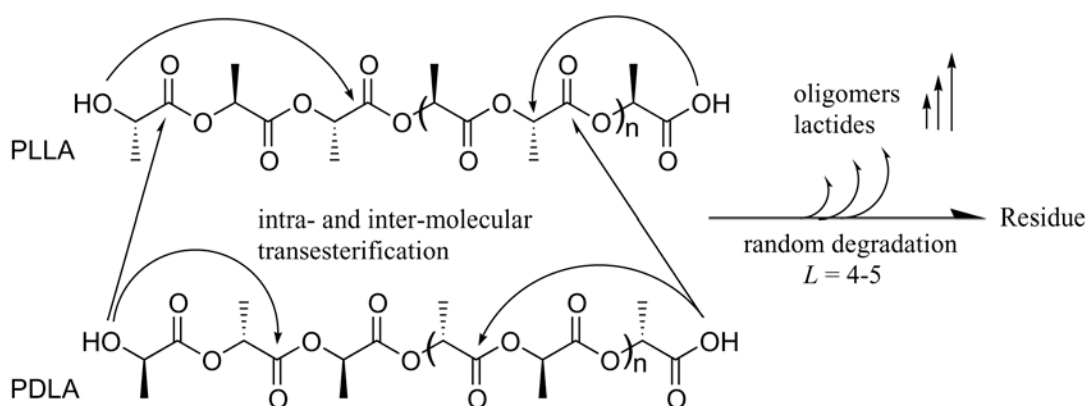
**Scheme 1.** Unzipping and transesterification reactions on scPLA-ap decomposition

Pyrolysis of scPLA-pr also proceeded mainly through the zero-order weight loss process as shown in Figure 6. The pyrolyzates were composed of dominant lactides and a small amount of cyclic oligomers, which were detected at temperatures higher than 300 °C (Figure 9). The degradation behavior of scPLA-pr was very similar to the PLLA-pr pyrolysis behavior. Thus, the Sn-catalyzed selective lactide elimination mechanism is expected to be a main mechanism for scPLA-pr pyrolysis, which was previously proposed for the PLLA-pr pyrolysis (Scheme 2) [29]. In this pyrolysis process, bimolecular transesterification reactions are also expected to be occurring on Sn atoms, because of the considerable formation of *meso*-lactide at the later stage of the pyrolysis. Further, similar intra-molecular transesterification should cause the formation of cyclic oligomers as

shown in Figure 9.



**Scheme 2.** Selective lactide elimination on scPLA-pr decomposition



**Scheme 3.** Random degradation reactions on scPLA-H decomposition

The pyrolysis of scPLA-H proceeded mainly through the random degradation ( $L = 4$ ) in the same way as the purified PLLA-H pyrolysis [26,28,29]. Particularly, the formation of a large amount of *meso*-lactide and diastereoisomers of cyclic oligomers in Figure 8 means that the inter-molecular transesterification often occurred during the scPLA-H pyrolysis. This production of cyclic oligomers, consisting of diastereoisomers, will be due to the random reactions caused by the hydroxyl and carboxyl end groups, and the ester-semiacetal tautomerization occurring at temperatures above 300°C (Scheme 3) [22].

## Conclusion

To clarify the pyrolysis behavior of PLA stereocomplex (scPLA), the scPLA samples with

different chain end structures, namely, as-polymerized scPLA-ap, precipitated-with-methanol scPLA-pr, and purified metal free scPLA-H, were prepared. The stereocomplex crystal made the starting temperature of the thermal degradation rise to around  $T_m$  (220 °C). Though the pyrolyzates from scPLA-ap and scPLA-pr were predominantly L,L-/D,D-lactides, a relatively large amount of *meso*-lactide formation was detected in the later stage of pyrolysis compared to those of the corresponding PLLAs, suggesting inter-molecular transesterification reactions occurred between PLLA and PDLA chains. From the analyses of dynamic TG data and the pyrolyzates, typical degradation mechanisms of these scPLAs were proposed as follows: unzipping depolymerization from Sn-alkoxide chain ends along with minor inter-molecular transesterification reactions, Sn-catalyzed selective lactide elimination and minor inter-molecular transesterification reactions, and random degradation ( $L = 4-5$ ) at higher temperatures for scPLA-ap, scPLA-pr, and scPLA-H, respectively. These degradation mechanisms were nearly the same as those of the corresponding PLLA samples.

### Acknowledgement

This study was financially supported by Special Coordination Funds of the Ministry of Education, Culture, Sports, Science and Technology, and the Japanese Government.

### Reference

- [1] Ikada Y, Tsuji H. Biodegradable polyesters for medical and ecological applications. *Macromol Rapid Commun* 2000;21:117-32.
- [2] Amass W, Amass A, Tighe B. A review of biodegradable polymers: Uses, current developments in the synthesis and characterization of biodegradable polyesters, blends of biodegradable polymers and recent advances in biodegradation studies. *Polym Int* 1998;47(2):89-144.
- [3] Anderson JM, Shive MS. Biodegradation and biocompatibility of PLA and PLGA microspheres. *Advan Drug Delivery Rev* 1997;28(1):5-24.
- [4] Ajioka M, Enomoto K, Suzuki K, Yamaguchi A. The basic properties of poly (lactic acid) produced by the direct condensation polymerization of lactic acid. *J Environ Polym Degrad* 1995;3:225-34.
- [5] Urayama H, Ohara H. Crystallinity and molding properties of polylactic acid (Lacty®). *Shimadzu Hyoron* 2000;56:163-8.
- [6] Tuominen J, Kylma J, Kapanen A, Venelampi O, Itavaara M, Seppala J. Biodegradation of lactic acid based polymers under controlled composting conditions and evaluation of the ecotoxicological impact. *Biomacromolecules* 2002;3:445-55.
- [7] Lunt J. Large-scale production, properties and commercial applications of polylactic acid polymers. *Polym Degrad Stab* 1998;59:145-52.
- [8] Migliaresi C, Cohn D, Lollis DE, Fameri L. Dynamic mechanical and calorimetric analysis of compression-molded PLLA of different molecular weights: effect of thermal treatments. *J Appl Polym Sci* 1991;43:83-95.
- [9] Ikada Y, Jamshidi K, Tsuji H, Hyon SH. Stereocomplex formation between enantiomeric poly(lactides). *Macromolecules* 1987;20:904-06.
- [10] Murdock JR, Loomis G.L. US Patent 4 719 246, 1988; US Patent 4 766 182, 1988; US Patent 4 800 219, 1989.
- [11] Tsuji H, Horii F, Hyon SH, Ikada Y. Stereocomplex formation between enantiomeric

- poly(lactic acid)s. 2. Stereocomplex formation in concentrated solutions. *Macromolecules* 1991;24:2719-24.
- [12] Tsuji H, Hyon SH, Ikada Y. Stereocomplex formation between enantiomeric poly(lactic acids). 5. Calorimetric and morphological studies on the stereocomplex formed in acetonitrile solution. *Macromolecules* 1992;25:2940-46.
- [13] Tsuji H, Ikada Y. Stereocomplex formation between enantiomeric poly(lactic acid)s. 6. Binary blends from copolymers. *Macromolecules* 1992;25:5719-23.
- [14] Radano CP, Baker GL, Smith MR. Stereoselective polymerization of a racemic Monomer with a racemic Catalyst: direct preparation of the polylactic acid stereocomplex from racemic lactide. *J Am Chem Soc* 2000;122:1552-3.
- [15] Nomura N, Ishii R, Akakura M, Aoi K. Stereoselective ring-opening polymerization of racemic lactide using aluminum-achiral ligand complexes: Exploration of a chain-end control mechanism. *J Am Chem Soc* 2002;124:5938-9.
- [16] Eling B, Gogolewski S, Pennings AJ. Biodegradable materials of poly(L-lactic acid): 1. Melt-spun and solution-spun fibres. *Polymer* 1982;23:1587-93.
- [17] Sodergard A, Nasman JH. Stabilization of poly(-lactide) in the melt. *Polym Degrad Stabi* 1994;46:25-30.
- [18] Wachsen O, Reichert KH. Thermal degradation of poly-L-lactide—studies on kinetics, modelling and melt stabilization. *Polym Degrad Stabi* 1997;57:87-94.
- [19] McNeill IC, Leiper HA. Degradation studies of some polyesters and polycarbonates-1. Polylactide: General features of the degradation under programmed heating conditions. *Polym Degrad Stab* 1985;11:267-85.
- [20] Leiper HA, McNeill IC. Degradation studies of some polyesters and polycarbonates-2. Polylactide: Degradation under isothermal conditions, thermal degradation mechanism and photolysis of the polymer. *Polym Degrad Stab* 1985;11:309-26.
- [21] Kopinke, FD, Mackenzie K. Mechanism aspects of the thermal degradation of poly(lactic acid) and poly (2-hydroxybutyric acid). *J Anal Appl Pyrolysis* 1997;40-41:43-53.
- [22] Kopinke FD, Remmler M, Mackenzie K, Moder M, Wachsen O. Thermal decomposition of biodegradable polyesters-II. Poly (lactic acid). *Polym Degrad Stab* 1996;53:329-42.
- [23] Cam D, Marucci M. Influence of residual monomers and metals on poly (L-lactide) thermal stability. *Polymer* 1997;38:1879-84.
- [24] Babanalbandi A, Hill DJT, Hunter DS, Kettle L. Thermal stability of poly(lactic acid) before and after <sup>3</sup>-radiolysis. *Polym Int* 1999;48:980-4.
- [25] Aoyagi Y, Yamashita K, Doi Y. Thermal degradation of poly[(R)-3-hydroxybutyrate], poly [μ-caprolactone], and poly[(S)-lactide]. *Polym Degrad Stab* 2002;76:53-9.
- [26] Fan Y, Nishida H, Hoshihara S, Shirai Y, Tokiwa Y, Endo T. Pyrolysis Kinetics of Poly(L-lactide) with Carboxyl and Calcium Salt End Structures. *Polym Degrad Stab* 2003;79:547-62.
- [27] Fan Y, Nishida H, Shirai Y, Tokiwa Y, Endo T. Racemization on Thermal Degradation of Poly(L-lactide) with Calcium Salt End Structure. *Polym Degrad Stab* 2003;80:503-11.
- [28] Nishida H, Mori T, Hoshihara S, Fan Y, Shirai Y, Endo T. Effect of tin on poly(L-lactic acid) pyrolysis. *Polym Degrad Stab* 2003;81:515-23.
- [29] Mori T, Nishida H, Shirai Y, Endo T. Effects of chain end structures on pyrolysis of poly(L-lactic acid) containing tin atoms. *Polym Degrad Stab*, in press.
- [30] Witzke DR, Narayan R, Kolstad JJ. Reversible kinetics and thermodynamics of the homopolymerization of L-lactide with 2-ethylhexanoic acid tin(II) salt. *Macromolecules* 1997;30:7075-85.
- [31] Shinno K, Miyamoto M, Kimura Y, Hirai Y, Yoshitome H. Solid-state postpolymerization of L-lactide promoted by crystallization of product polymer: An effective method for reduction of remaining monomer. *Macromolecules* 1997;30:6438-44.
- [32] Kowalski A, Duda A, Penczek S. Kinetics and mechanism of cyclic esters polymerization initiated with tin(II) octoate. 3. Polymerization of L,L-dilactide. *Macromolecules* 2000;33:7359-70.
- [33] Kowalski A, Libiszowski J, Duda A, Penczek S. Polymerization of L,L-dilactide initiated by

- tin(II) butoxide. *Macromolecules* 2000;33:1964-71.
- [34] Zhang X, Wyss UP, Pichora D, Goosen MFA. An investigation of the synthesis and thermal stability of poly(DL-lactide). *Polym Bull* 1992;27:623-9.
- [35] Schwach G, Coudane J, Engel R, Vert M. Zn lactate as initiator of DL-lactide ring opening polymerization and comparison with Sn octoate. *Polym Bull* 1996;37:771-6.
- [36] Doyle CD. Estimating isothermal life from thermogravimetric data. *J Appl Polym Sci* 1962;6:639-42.
- [37] Reich L. A rapid estimation of activation energy from thermogravimetric traces. *Polym Lett* 1964;2:621-3.
- [38] Ozawa T. A new method of analyzing thermogravimetric data. *Bull Chem Soc Japan* 1965;38:1881-6.
- [39] Nishida H, Yamashita M, Hattori N, Endo T, Tokiwa Y. Thermal decomposition of poly(1,4-dioxan-2-one). *Polym Degrad Stab* 2000;78:485-96.
- [40] Doyle CD. Kinetics analysis of thermogravimetric data. *J Appl Polym Sci* 1961;5:285-92.
- [41] Wachsen O, Platkowski K, Reichert KH. Thermal degradation of poly-L-lactide – studies on kinetics, modeling and melt stabilization. *Polym Degrad Stab* 1997;57:87-94.
- [42] Flynn JH, Wall LA. General treatment of the thermogravimetry of polymers. *J Res Nat Bur Stand* 1966;70A:487-523.
- [43] Nishida H, Yamashita M, Endo T. Analysis of initial process in pyrolysis of poly (*p*-dioxanone). *Polym Degrad Stab* 2002;78:129-135.
- [44] Khabbaz F, Karlsson S, Albertsson AC. Py-GC/MS an effective technique to characterizing of degradation mechanism of poly (L-lactide) in the different environment. *J Appl Polym Sci* 2000;78:2369-78.
- [45] Westphal C, Perrot C, Karlsson S. Py-GC/MS as a means to predict degree of degradation by giving microstructural changes modeled on LDPE and PLA. *Polym Degrad Stab* 2001;73:281-7.
- [46] Duda A, Penczek S. Thermodynamics of L-lactide polymerization. Equilibrium monomer concentration. *Macromolecules* 1991;23:1636-9.
- [47] Kricheldorf HR, Kreiser-Saunders I, Boettcher C. Polylactones: 31. Sn(II) octoate-initiated polymerization of L-lactide: a mechanistic study. *Polymer* 1995;36:1253-9.